

Journal of Hydraulic and Water Engineering (JHWE)



Journal homepage: https://jhwe.shahroodut.ac.ir

Optimizing Organic Dye Degradation via Electro-Peroxone Process: An Experimental and Machine Learning Approach

Seyedeh Fatemeh Khakzad¹, Tahere Taghizade Firozjaee^{1,*}, Jafar Abdi²

Article Info

Article history:
Received 03 July 2025
Received in revised form 06
September 2025
Accepted 16 September 2025
Published online 22 September 2025

DOI: 10.22044/JHWE.2025.16466.1071

Keywords

Electroperoxone
Degradation
Machine learning
Experimental optimization
Advanced oxidation processes.

Abstract

electroperoxone (EPO) process, which integrates electrochemical hydrogen peroxide generation, has attracted attention as an efficient advanced oxidation technology for treating recalcitrant pollutants. This study investigates the application of EPO for the removal of organic dye from synthetic wastewater using a two-stage analytical framework. In the first stage, a series of systematic batch experiments were conducted to investigate the effects of key operational parameters initial pH, applied current, ozone dosage, and reaction time on decolorization efficiency. In the second stage, predictive models were developed using machine learning algorithms Support Vector Regression (SVR) and Random Forest (RF) to capture the process's complex, nonlinear behavior. The Random Forest model outperformed others, achieving an R² value above 0.823 and demonstrating superior accuracy in predicting removal efficiency. Sensitivity analysis revealed ozone dosage and applied current as the most influential factors. These results highlight the potential of combining experimental optimization with robust data-driven modeling to enhance the design and scalability of advanced oxidation processes in wastewater treatment.

1. Introduction

In recent decades, the escalating contamination of water resources by a myriad of industrial chemicals and toxic substances has emerged as a paramount global challenge. (Deogaonkar-Baride et al., 2025; Firozjaee et al., 2020). The discharge of inadequately treated effluents from various sectors, particularly the textile industry, introduces a complex mixture of hazardous compounds into aquatic ecosystems, jeopardizing both environmental integrity and public health (Bopape et al., 2024).

Azo dyes are among the most persistent organic pollutants in aquatic environments, posing

significant environmental and health concerns due to their stability and resistance to conventional degradation processes (Srivatsav, Devi et al.). Methyl orange (MO), a widely used azo dye, is particularly recalcitrant under natural conditions, leading to long-term accumulation in water bodies and potential toxic effects on aquatic ecosystems. The presence of such pollutants highlights the need efficient and sustainable removal technologies that can effectively degrade these contaminants into less harmful byproducts(Tamer et al., 2024; Tingting et al., 2015).

¹Department of Water and Environmental Engineering, Faculty of Civil Engineering, Shahrood University of Technology, Shahrood, Iran

²Department of Chemical Engineering, Faculty of Chemical and Materials Engineering, Shahrood University of Technology, Shahrood, Iran

^{*} Corresponding author: t.taghizade@shahroodut.ac.ir, Tel:+989101001159

Advanced oxidation processes (AOPs) have extensively investigated for degradation of recalcitrant organic pollutants due to their ability to generate highly reactive species that facilitate the breakdown of complex molecular structures(Abdi et al., 2025; Chaturvedi et al., 2022; Shahamat et al., 2022). Among these, the electroperoxone (EPO) process, which integrates electrochemical oxidation with ozonation, has emerged as a promising technique for removing azo dyes from wastewater(Chen et al., 2023). The effectiveness of this process is influenced by several operational parameters, including electrolyte concentration, pH, ozone dosage, and initial pollutant concentration, which collectively determine its overall performance(Chen et al., 2023; Shokri & Sanavi Fard, 2022).

Despite the demonstrated efficiency of AOPs, optimizing their operational conditions remains challenging due to complex interactions among process variables. Traditional experimental approaches for process optimization are often time-intensive resource-demanding, and limiting their practical applicability in largescale treatment systems(Liu et al., 2024). In recent years, machine learning techniques have been increasingly applied to environmental modeling, offering a data-driven process optimization approach to predictive analysis. Various ML algorithms, including support vector regression (SVR) and random forest (RF) have been employed to enhance the accuracy of pollutant degradation predictions and provide valuable insights into process dynamics(Fahimi Bandpey et al., 2024; Lateef et al., 2022; Moosavi et al., 2021; Saghafi et al., 2024).

In this study, we investigate the removal of MO using the EPO process and employ ML models to predict and optimize its degradation efficiency. The predictive performance of different ML algorithms is evaluated based on standard statistical metrics, including mean absolute error (MAE) and the coefficient of determination (R^2) . By integrating experimental findings with data-driven modeling, this study aims to provide a robust framework for improving AOPs and advancing sustainable water treatment technologies.

2. Materials and Methods

2.1. Experimental

2.1.1. Materials

Methyl orange (MO, $C_{14}H_{14}N_3NaO_3S$), used as the model organic contaminant in this study, was obtained from Merck Co. (Germany) with a purity greater than 99%. Sodium sulfate $(Na_2SO_4, Merck)$ was used as the supporting electrolyte to provide ionic conductivity during electrochemical treatment. pH adjustments were performed using 37% hydrochloric acid (HCl) and sodium hydroxide (NaOH), both purchased from Merck. All solutions were prepared using deionized water to eliminate the influence of background ions. Graphite plates (99.9% purity) were used as the cathodic electrode material due to their high electrical conductivity, chemical stability, and costeffectiveness.

2.1.2. Experimental Set-up

A schematic of the experimental setup is presented in Fig. 1a. The system consists of an oxygen capsule (1), an ozone generator (2), a programmable DC power supply (3), a magnetic stirrer (4), and a borosilicate glass reactor (5) with an effective working volume of 75 mL. Oxygen gas was passed through the ozone generator, where it was partially converted to ozone. The resulting ozone—oxygen mixture was then introduced directly into the reactor to enhance the oxidative degradation of the target pollutant.

The internal structure of the reactor is shown in Fig. 1b. Two flat electrodes were positioned vertically and 1 cm apart inside the reactor: a graphite plate $(3 \times 4 \text{ cm}^2)$ served as the cathode, and a steel sheet of the same size functioned as the anode. Before each experiment, the electrodes were polished with fine sandpaper, immersed in 10% nitric acid for chemical cleaning, rinsed with deionized water, and dried at room temperature to ensure consistent surface conditions.

The reactor was placed on a magnetic stirrer operating at 500 rpm to ensure continuous

mixing of the electrolyte and uniform distribution of oxidants. A constant electric current was applied via the DC power supply. All experiments were performed at ambient temperature $(25\pm1~^{\circ}\text{C})$ under galvanostatic conditions.

A 0.025 mol/l sodium sulfate (Na_2SO_4) solution was used as the supporting electrolyte. When necessary, the pH of the solution was adjusted using dilute hydrochloric acid (HCl) or sodium hydroxide (NaOH). In this combined system, ozone is introduced into the aqueous phase, while hydrogen peroxide (H_2O_2) is generated electrochemically at the cathode surface through the reduction of dissolved oxygen. These two oxidants interact through the peroxone reaction, producing highly reactive hydroxyl radicals (•OH), which are the primary agents responsible for the degradation of methyl orange. Additionally, ozone can decompose directly in water, especially under slightly alkaline conditions, further contributing to OH• formation. These radicals initiate non-selective oxidation, breaking azo bonds and aromatic rings, and leading to the

2.1.3. Research Methods

According to the preliminary studies, the investigated parameters were determined according to Table 1(Ghalebizade & Ayati, 2016; Naseri & Ayati, 2024).

Table 1. The range of tested parameters.

Parameter	Value	Unit	
Methyl Orange Concentration	10-50-100	ppm	
pН	3-5-7-8-9	-	
O ₃ Rate	0.26 - 0.36 - 0.42	gr/h	
Na2So4	0.025-0.05-	Molar	
Concentration	0.075-0.1		
Intensity	250-500- 1000	mA	

To determine various concentrations of methyl orange, its UV-Vis absorption spectrum was used. The elimination rate of the methyl orange contaminant was measured using a spectrophotometer at its peak absorption wavelength (464 nm), and

mineralization of dye molecules into CO_2 , H_2O , and inorganic ions. The overall mechanism of radical generation and pollutant breakdown is depicted in Figure 1b, which illustrates the synergy between ozone delivery and electrochemical H_2O_2 production within the reactor.

To monitor the degradation process, 3 mL samples were taken from the reactor at 10minute intervals. Each sample was filtered through a 0.45 µm membrane filter and analyzed using a UV-Vis spectrophotometer (Hach DR6000, Germany) at the maximum absorbance wavelength of methyl orange (464 nm). All experiments were conducted in triplicate, and the results are presented as mean ± standard deviation to ensure data reliability. A schematic timeline of the experimental procedure is provided in Figure 1c, illustrating the sequence of steps from solution preparation to ozone generation, EPO setup, time-based sampling, and final analysis. This visual guide complements the equipment schematic (Figure 1a-b) and helps clarify the practical flow of the experiments.

the efficiency of pollutant removal was calculated using Eq. (1).

$$RE(\%) = \frac{C_0 - C}{C_0} \times 100$$
 (1)

Where C_0 and C are the initial and final dye concentration (mg/l), respectively.

2.1.4. Energy Consumption Calculation

To assess the sustainability of the Electro-Peroxone (EPO) process, the specific energy consumption (EC) was calculated under the optimal operational conditions. Energy consumption reflects the amount of electrical energy required to degrade a unit mass of the target pollutant and is a key indicator of process feasibility, particularly for scaling to industrial applications.

The energy consumption (in Wh/g of dye removed) was calculated using equation (2):

$$EC = \frac{U \times I \times t}{C_{Removed}} \tag{2}$$

Where: U is the applied voltage (V), I is the applied current (A), t is the total reaction time (h), $C_{Removed}$ is the mass of dye removed (g), which was calculated from the initial dye concentration, solution volume, and removal efficiency.

2.2. Machine Learning Prediction 2.2.1. Dataset

The dataset used for machine learning model generated from a development was comprehensive set of 205 batch experiments performed under diverse operating conditions. Each experiment was designed by varying key process parameters including initial pH, current intensity, ozone flow rate, electrolyte concentration, and initial dye concentration—to evaluate their influence on the degradation efficiency of methyl orange. The output variable for each data point was the removal efficiency (%), determined via UV-Vis spectrophotometry at 464 nm.

The range and levels of the experimental variables are detailed in Table 1. This dataset captures complex, nonlinear interactions between process parameters, providing a robust basis for machine learning model development.

Prior to modeling, the dataset was randomly shuffled and split into 80:20 train/test, with 164 data points for training and 41 for testing. All input features were normalized using Min-Max scaling to ensure they were comparable on a numerical scale. Additionally, five-fold cross-validation was employed on the training set during hyperparameter tuning to improve model generalization and reduce the risk of overfitting.

Data preprocessing, model development, and performance evaluation were performed using Python 3.11 and the scikit-learn

(v1.4.2) library, along with NumPy and pandas for numerical and data handling tasks.

This structured dataset served as the foundation for training and evaluating Support Vector Regression (SVR) and Random Forest Regression (RFR) models to predict methyl orange removal efficiency with high accuracy and reliability.

Figure 2 presents a flowchart of the full machine learning prediction pipeline.

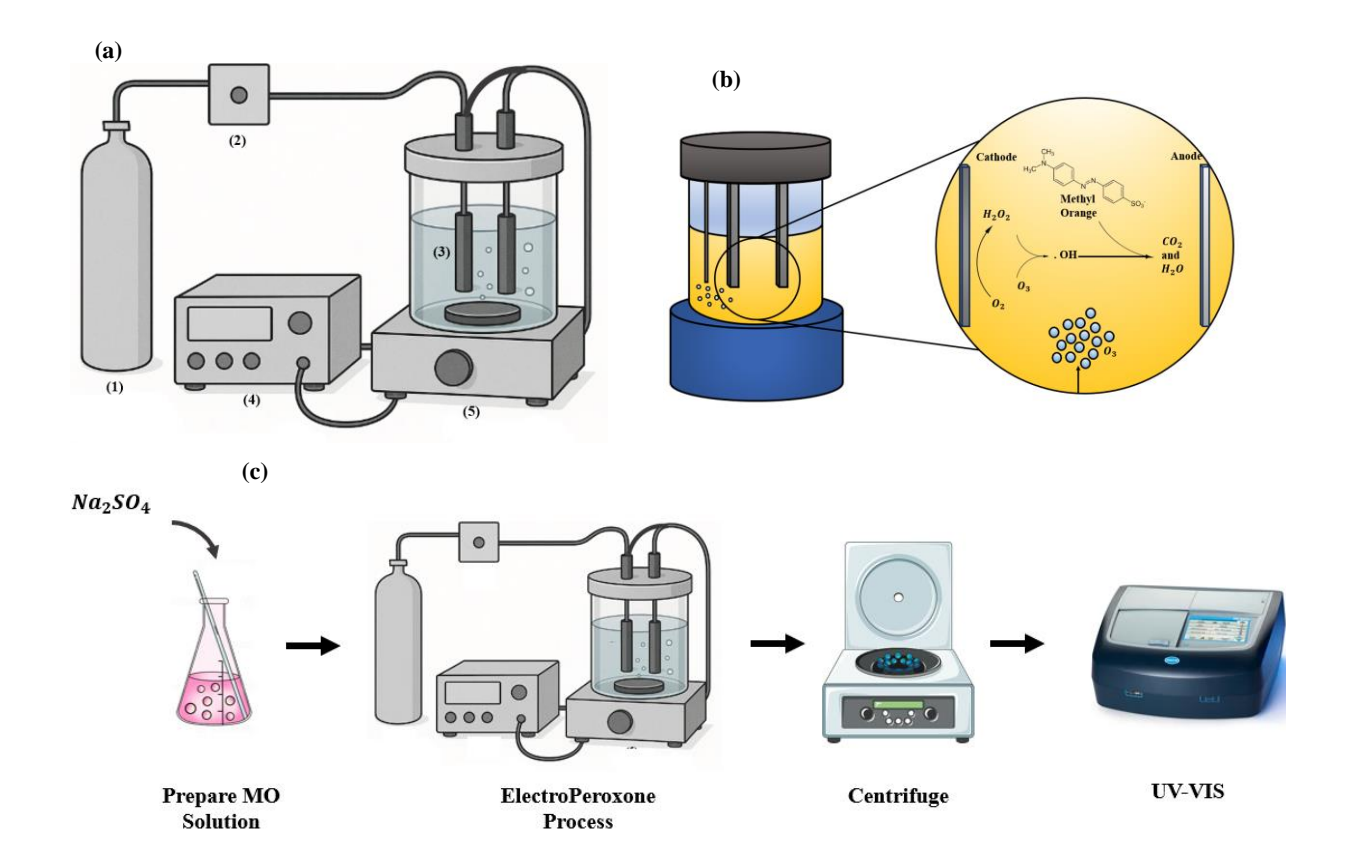


Figure 1. (a) Overall system layout: (1) oxygen capsule, (2) ozone generator, (3) borosilicate glass reactor (100 mL), (4) programmable DC power supply, and (5) magnetic stirrer., (b) Internal structure of the reactor, showing the graphite cathode and platinum anode (both 3×4 cm²), and (c) schematic overview of the experimental procedure including solution preparation, EPO setup, sampling, and result analysis.

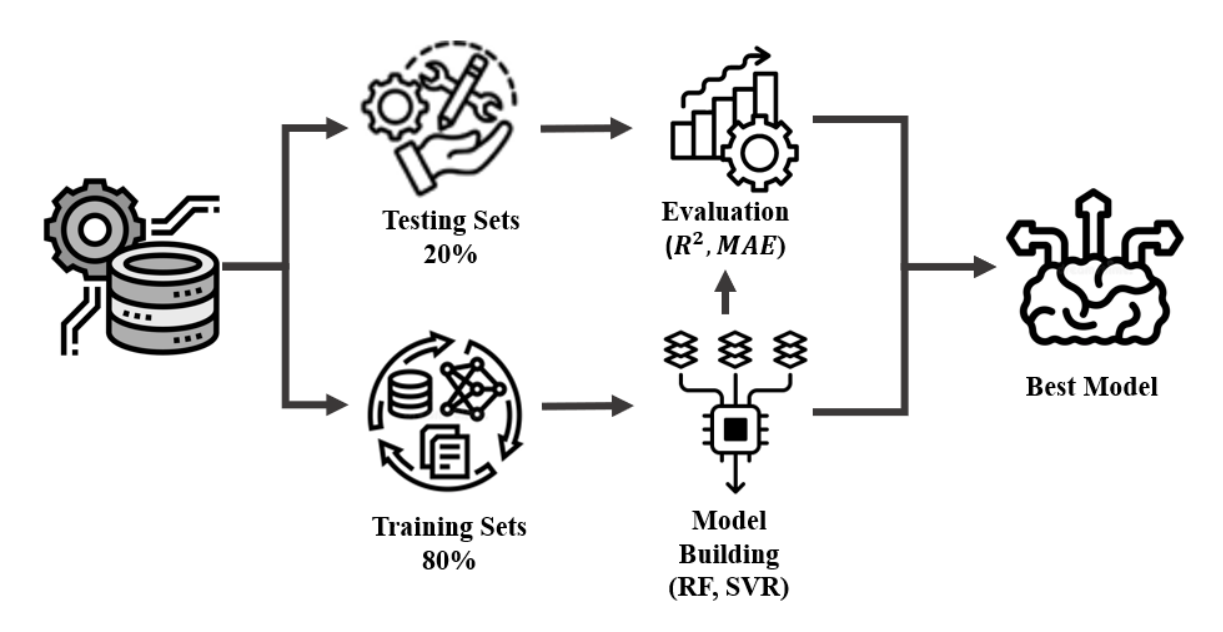


Figure 2. Prediction process in machine learning systems.

2.2.2. Support Vector Regression (SVR)

The Support Vector Regression (SVR) algorithm is a method grounded in Support Vector Machine (SVM) theory and is commonly used for modeling complex, nonlinear relationships in regression problems. The main idea behind SVR is to construct an optimal hyperplane within the feature space that keeps prediction errors within a certain acceptable range, known as epsilon.

Unlike traditional regression approaches that focus on minimizing absolute or squared errors, SVR seeks a function that stays within this defined tolerance zone—without overreacting to data points outside it. During the learning process, SVR first maps the input data into a higher-dimensional space to better capture non-linear patterns. This is typically done using kernel functions such as linear, polynomial, or Gaussian (RBF) kernels.

Once transformed, the model creates two boundary hyperplanes designed to contain most of the data points. Any point outside this zone is treated as a support vector, which influences the final structure of the regression function. The optimization process in SVR minimizes a cost function that penalizes data points that fall outside the epsilon margin.

Key parameters in this model include C, which controls the penalty for errors outside the margin, and ϵ (epsilon), which sets the

allowable range for prediction deviation. Finding the right balance between these parameters is essential to manage model complexity and to prevent both overfitting and underfitting

2.2.3. Random Forest (RF)

Random Forest is an ensemble-based machine learning algorithm that uses a collection of decision trees to make predictions. As shown in Fig. 3, each tree is built independently, and the final prediction is obtained by either voting (for classification tasks) or averaging the outputs (for regression tasks) across all trees. This approach is especially effective in reducing overfitting and improving model accuracy when dealing with complex datasets.

A key feature of Random Forest is its use of randomness—both in selecting subsets of data and features for each tree—and its ability to estimate feature importance using advanced techniques. The model's main parameters include n_estimators (the number of trees in the forest) and max_depth (the maximum depth of each tree), both of which significantly influence the model's accuracy and complexity.

Random Forests are widely applied to both regression and classification problems, particularly when handling noisy or highly complex data.

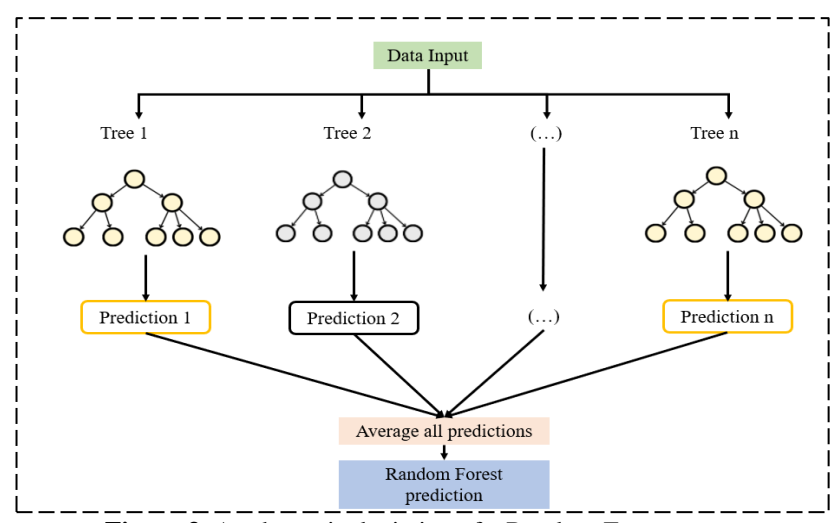


Figure 3. A schematic depiction of a Random Forest netwo

2.2.4. Evaluation Metrics

To assess the predictive performance of the developed machine learning models, including Support Vector Regression (SVR) and Random Forest Regression (RFR), two widely used statistical metrics were employed: Mean Absolute Error (MAE) and the coefficient of determination (R²). These metrics provide complementary insights into model accuracy and generalization ability.

The MAE measures the average magnitude of the prediction errors, providing a direct measure of the model's deviation from the actual values, independent of their direction. It is defined in equation (3):

$$MAE = \frac{1}{n} \sum_{i=1}^{n} |y_i - \widehat{y}_i|$$
(3)

Where y_i and y_i enote the actual and predicted values, respectively, and n is the number of observations.

The R² score, also known as the coefficient of determination, indicates the proportion of the variance in the dependent variable that is predictable from the independent variables. It is given by equation (4):

$$R^{2} = 1 - \frac{\sum_{i=1}^{n} (y_{i} - \widehat{y}_{i})^{2}}{\sum_{i=1}^{n} (y_{i} - \overline{y}_{i})^{2}}$$
(4)

Where $\overline{y_l}$ is the mean of the actual values. An R^2 value closer to 1 signifies better model performance, while values near or below zero indicate poor predictive capability.

All models were trained and validated using the same dataset split to ensure a fair comparison. Hyperparameters for both SVR and RFR models were optimized using grid search with k-fold cross-validation (k = 5), h may favor undesired reactions over oxygen evolution(Khataee et al., 2011; Naseri & Ayati, 2024).

Interestingly, at 250 mA, the dye removal efficiency reaches nearly 99% within 20 minutes and remains stable throughout the reaction. This suggests that lower current intensity not only achieves high removal

ensuring robustness and reducing the risk of overfitting. Model evaluation was performed on the holdout (test) dataset, which was not exposed during training.

3. Results and Discussions3.1. Effect of Current Intensity

The effect of applied current on process performance is illustrated in Fig. 4. As shown, increasing the applied current from 250 mA to 500 mA significantly enhances the dye removal efficiency, from approximately 68% to 94% after 20 minutes of reaction time. This enhancement is attributed to the higher production of hydrogen peroxide at the cathode surface with increasing current intensity, which leads to a greater generation of hydroxyl radicals with powerful oxidizing agents responsible pollutant for degradation(Ghalebizade & Ayati, 2016; Ghasemi et al., 2020)...

A further increase in current intensity to 1000 mA results in a slight improvement in dye removal, reaching around 97%. However, the enhancement beyond 500 mA is marginal, and the efficiency appears to plateau. This indicates that the production of hydroxyl radicals may have reached a saturation point due to limited ozone solubility in the aqueous medium, thereby preventing additional radical formation despite the higher current input. Moreover, the excess hydrogen peroxide generated at elevated current levels could act as a scavenger for hydroxyl radicals, reducing their availability through parasitic side reactions. Another possible explanation for the decreased efficiency at 1000 mA is the decomposition or reduction of hydrogen peroxide at the cathode surface due to the increased applied potential.

efficiency but also maintains it consistently, likely with lower energy consumption. Thus, it can be concluded that 250 mA represents the optimal current intensity in this system, offering both high efficiency and better energy economy.

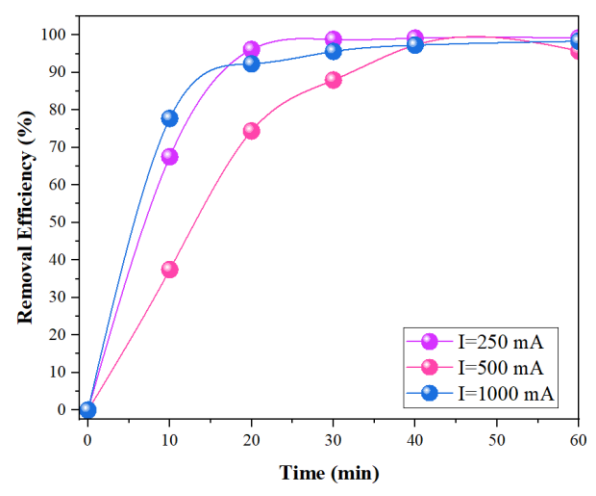


Figure 4. Effect of Current Intensity on dye removal efficiency (Experimental conditions: Initial dye concentration = 50 ppm, Electrolyte concentration = 0.025 M, Ozone flow rate = 0.2 gr/h, pH = 6.4).

3.2. Effect of Electrolyte Concentration and Ozone Flow

Electrolyte concentration plays a pivotal role in modulating electrochemical oxidation efficiency, primarily by influencing ionic conductivity, interfacial charge-transfer kinetics, and reactive species formation. Sodium sulfate (Na_2SO_4), a widely used inert electrolyte in electrochemical advanced oxidation processes (EAOPs), was selected to evaluate the role of supporting electrolyte concentration in the degradation of methyl orange.

Experiments were conducted using four Na_2SO_4 concentrations (0.025, 0.05, and 0.1 M), and their effects on dye removal efficiency were assessed over 60 minutes (Fig. 5). As observed, increasing electrolyte concentration from 0.025 M to 0.1 M generally enhanced the degradation rate, with initial removal efficiency at 20 minutes rising from ~78% to ~93%. This enhancement is attributed to a reduction in ohmic resistance, which facilitates electron transfer and promotes in situ generation of H_2O_2 via the two-electron reduction of oxygen at the cathode(Naseri & Ayati, 2024).

However, a more complex interplay emerges at higher electrolyte concentrations. While 0.1 M demonstrated superior early-stage performance, it plateaued at ~96% removal

by 60 minutes, slightly lower than the 98% and 97% achieved at 0.05 respectively. This non-linear trend may be attributed to side reactions and radical scavenging phenomena. At elevated sulfate concentrations, excessive SO_4^{2-} can competitively react with hydroxyl radicals (•OH), forming sulfate radicals ($SO_4 \bullet -$).

While $SO_4 \bullet^-$ is a potent oxidant ($E^0 \approx 2.6 \, V$), its selectivity and reaction kinetics differ significantly from those of (\bullet OH), possibly leading to less effective dye mineralization or recombination losses. Furthermore, an overabundance of ionic species can suppress mass transport near the electrode interface or shift equilibrium reactions unfavorably.

Fig. 6 presents the effect of the injected ozone flow rate on the efficiency of the electroperoxone process for various ozone flow rates including 0.26 gr/h, 0.36 gr/h, and 0.42 gr/h. Increasing the injected ozone flow is associated with improved pollutant removal efficiency. So that, by increasing the ozone flow from 0.26 g/h to 0.42 g/h, the dye removal efficiency improves approximately 82% to 92% after 30 minutes. Increasing the injected ozone flow leads to an increased reaction of hydrogen peroxide and ozone and eventually the production of more hydroxyl radicals, which improves the dye removal efficiency(Wu et al., Increasing the amount of injected ozone enhances the transfer of ozone from the gas phase to the solution phase. Therefore, the reactions of ozone with hydrogen peroxide and the reduction of ozone at the cathode surface are improved. Based on the results presented in Fig. 6, increasing the injected ozone flow rate from 0.26 g/h to 0.42 g/h consistently enhanced the dye removal efficiency throughout the experiment.

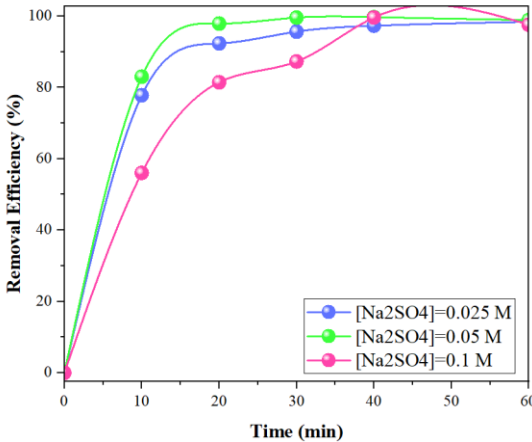


Figure 5. Effect of electrolyte concentration on dye removal efficiency (Initial dye concentration = 50 ppm, Ozone flow rate = 0.2 gr/h, Intensity = 1000 mA, pH =6.4).

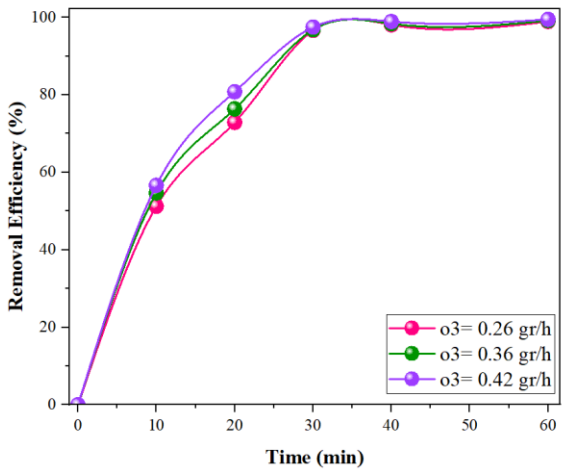


Figure 6. Effect of ozone flow rate on dye removal efficiency (Experimental conditions: Initial dye concentration = 50 ppm, Electrolyte concentration = 0.025 M, Intensity = 1000 ma, pH =6.4).

3.3. Effect of Initial pH

The effect of initial pH (3, 5, 7, 8, and 9) on the dye removal efficiency was studied under the optimum conditions obtained from previous experiments, as shown in Fig. 7. Primary pH values were adjusted but not controlled during the reaction.

The results presented in Fig. 6 indicate that the initial pH has a noticeable impact on the dye removal efficiency. The dye removal efficiency at the endpoint of the experiment at pH 3, 5, 7, 8, and 9 was approximately 98.8%, 97.9%, 93.6%, 88.2%, and 79.8%, respectively.

The electro-peroxone process in this study demonstrated higher dye removal efficiency under acidic conditions, consistent with the observed results. While ozonation sometimes reported to perform better in alkaline pH due to the formation of reactive radicals like hydroxyl radicals (•OH) from ozone and hydroxide ions, the actual efficiency can vary depending on the system. In acidic conditions, ozone remains more stable and reacts directly with the dye molecules, thereby enhancing degradation. Additionally, the presence of hydrogen peroxide at lower pH may promote radical formation without significant scavenging effects, resulting in improved dye removal efficiency at acidic pH levels(Ghasemi et al., 2020).

Another possible mechanism for hydroxyl radical production involves a reaction involving the basic form of hydrogen peroxide. Based on this reaction, the conjugate acid of hydrogen peroxide can react with ozone to produce hydroxyl radicals, which degrade contaminants.

The high efficiency of the electro-peroxone process observed in our experiments at an acidic pH (pH 3) might be related to a better performance of the electrode material in generating hydrogen peroxide under these conditions. The results show that the electroperoxone process exhibits relatively high efficiency across the tested pH range (3-9), although the dominant treatment mechanism might vary at different pH values. Other researchers acknowledge this complexity due to pH changes(Bakheet et al., 2013; Khataee et al., 2011). The overall results suggest that electro-peroxone process provides acceptable performance across a wide pH range. Given the high efficiency observed across different pH values in our study, using the natural pH of the dye solution may be optimal to minimize costs and issues associated with initial pH adjustment.

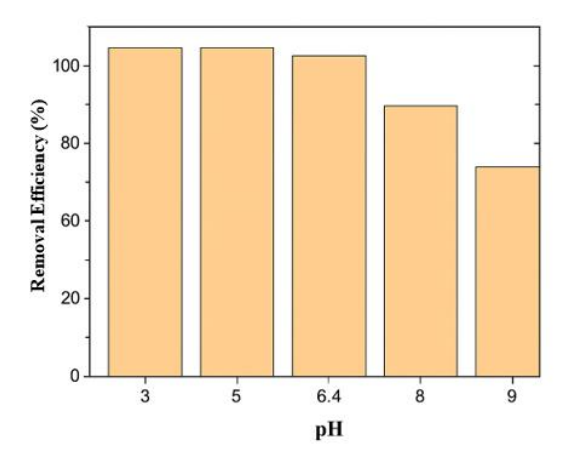


Figure 7. Effect of pH on dye removal efficiency (Initial dye concentration = 50 ppm, Ozone flow rate = 0.2 gr/h, Intensity = 1000 mA, Electrolyte concentration = 0.025 M).

3.4. Effect of Initial Dye Concentration

The effect of changes in the initial dye concentration on electro-peroxone efficiency is shown in Fig. 8. This figure illustrates the dye removal efficiency over time for three different initial dye concentrations: 10 ppm, 50 ppm, and 100 ppm.

The results in Fig. 6 indicate that the initial dye concentration has a noticeable impact on the reaction time required to achieve significant removal. As the initial dye concentration increases from 10 ppm to 50 ppm, then to 100 ppm, the time needed to achieve a high percentage of dye removal generally increases.

Specifically, at the lowest concentration of 10 ppm, a high removal efficiency (around 90%) is achieved relatively quickly, within approximately 25 minutes. When the initial concentration is increased to 50 ppm, a similar high removal efficiency (around 98%) is achieved, but it takes longer — approximately 40 minutes. The highest initial concentration tested, 100 ppm, shows a slightly slower initial removal rate than 50 ppm, but it reaches a high removal efficiency (around 98%) after approximately 50 minutes.

In electrochemical processes, increasing the concentration of contaminants can reduce removal efficiency or extend reaction time because the amount of oxidizing agents produced may remain relatively constant. In our experiments, a high dye removal efficiency is achieved across all tested initial concentrations. Still, the time required to reach that efficiency is clearly influenced by the initial dye load.

Considering these results, a lower initial pollutant concentration appears to lead to faster removal kinetics in our electroperoxone system. However, it's also essential to consider energy consumption per unit of removed dye, as discussed in the referenced text, to determine the most economically viable operating conditions for different initial concentrations. The trade-off between reaction time and energy efficiency often necessitates finding an optimal initial dye concentration for a given system.

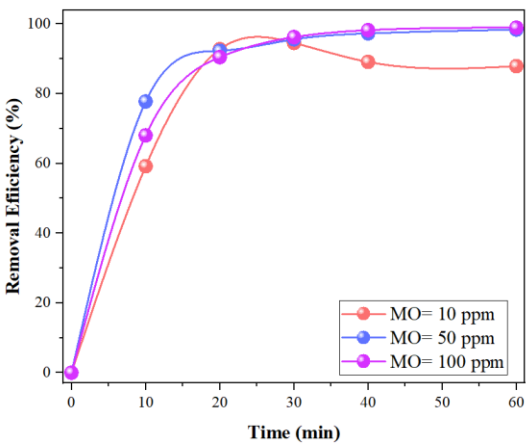


Figure 8. Effect of initial concentration on dye removal efficiency (pH = 6.4, Ozone flow rate = 0.2 gr/h, Intensity = 1000 mA, Electrolyte concentration = 0.025 M).

3.5. Energy Consumption Analysis

Under optimal operating conditions (30 V, 250 mA, 60 min), the system achieved 99% removal of 50 ppm MO from 75 mL solution. The total energy used was 7.5 Wh, corresponding to approximately 2,019.6 Wh per gram of dye removed. While this value may appear high due to the small reaction volume, it reflects the power intensity typical of lab-scale setups and can be optimized in scaled-up systems.

3.5 Predictive Modeling of Methyl Orange (MO) Removal Efficiency: Performance Assessment of SVR and Random Forest

To develop reliable predictive models for the electroperoxone-based removal of methyl orange (MO), two supervised machine learning algorithms—Support Vector Regression (SVR) and Random Forest (RF)—were investigated. Their performance was quantitatively compared using two key statistical metrics: the coefficient of determination (R²) and the mean absolute error (MAE), as summarized in Table 2.

3.5.1 Performance and Limitations of the SVR Model

The SVR model was implemented with a radial basis function (RBF) kernel, and the hyperparameters were optimized via a systematic grid search. The optimal setting $(C = 46.0, \varepsilon = 0.01)$ yielded an R² of 0.672 and a MAE of 8.49. These results indicate moderate accuracy in predicting MO removal efficiency. Although SVR captured general patterns in the dataset, its predictive variance increased notably at extreme values and complex nonlinear interactions, suggesting limited generalization capability. As shown in Figure 9, the SVR predictions deviated substantially from the identity line, especially for observations near operational boundaries. This discrepancy may stem from the model's sensitivity to outliers and its inability to fully accommodate the multivariate, nonlinear behavior inherent in electrochemical degradation processes.

3.5.2 Predictive Superiority of the Random Forest Model

In contrast, the Random Forest model demonstrated significantly better performance, achieving an R² of 0.823 and a lower MAE of 6.38 with only 6 decision trees (n_estimators = 6) and a fixed random state of 49. RF's ensemble learning structure, which aggregates outputs from multiple decorrelated decision trees, enables the

model to robustly learn from complex, noisy, and nonlinear data without extensive tuning. As illustrated in Figure 9, the RF model produced predictions that aligned more closely with the experimental data, showing minimal dispersion and improved consistency across the range of values. Figure 10 further supports this observation, showing that RF effectively tracked temporal or sample-based variations, minimizing both over- and under-estimations.

The superior performance of RF is attributed to its:

- Tolerance to overfitting via bootstrap aggregation,
- Capability to model higher-order interactions without requiring explicit functional forms,
- Reduced sensitivity to data distribution assumptions.

3.5.3 Model Comparison and Implications for Process Optimization

The comparative results (Table 2) highlight that RF outperformed SVR across all evaluation criteria. The R² value improved by approximately 24%, while the MAE decreased by nearly 25%. This substantial performance gain underscores RF's superior capacity to capture the inherent complexities of the electrochemical treatment system.

From an applied perspective, the Random Forest model holds greater promise for deployment practical in real-time environmental monitoring and process control applications. Its high accuracy, stability, and interpretability make it an excellent candidate for supporting decisionmaking frameworks in advanced oxidation processes particularly (AOPs), under dynamic and nonlinear operating conditions.

Table 2. Comparative performance of SVR and Random Forest models in predicting methyl orange removal efficiency

Model	Optimized Hyperparameters	R ²	MAE
SVR	C = 46.0, Epsilon = 0.01	0.672	8.49
Random Forest	n_estimators = 6, random_state = 49	0.823	6.38

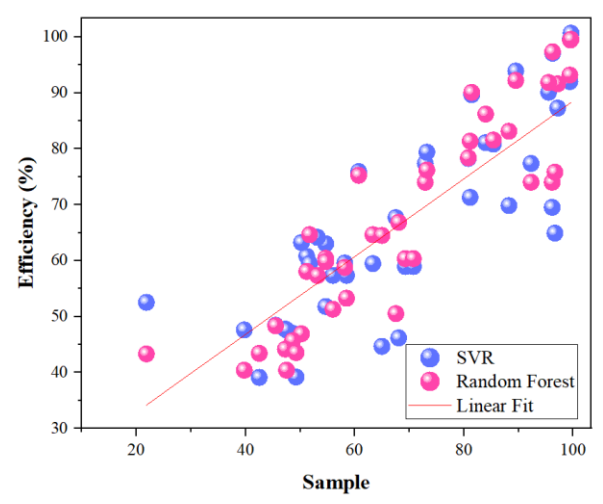


Figure 9. Comparison of predicted versus actual MO removal efficiency using SVR and Random Forest models.

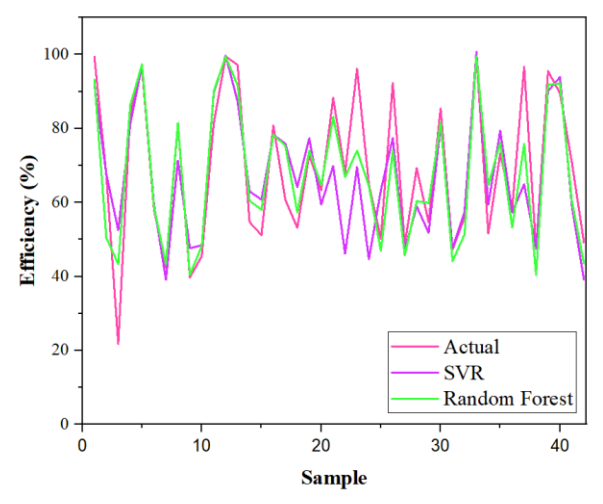


Figure 10. Trend analysis of actual versus predicted MO removal efficiencies across test samples.

4. Results and Discussion

4.1. Sustainability and Environmental Safety

In terms of sustainability and environmental safety, the post-treatment solution was neutralized and filtered, and excess ozone was quenched using KI solution. While the supporting electrolyte (sodium sulfate) is

inert, further work is needed to evaluate potential trace by-products and to explore safe reuse or disposal of treated effluents in real applications.

4.2. Study Limitations

It is also essential to acknowledge some practical limitations. This study used synthetic dye solutions, which enabled precise control of variables and reproducibility. However, real wastewater contains a broader and more complex matrix that may affect performance. Moreover, although the experiments lasted only 60 minutes, the stable removal efficiency observed suggests good short-term Future reliability. investigations recommended to explore longer operation times (e.g., 120-180 minutes), evaluate electrode longevity, assess fouling behavior, and confirm the system's robustness in repeated or continuous operation.

5. Conclusions

This study demonstrated the effective degradation of methyl orange (MO) using the electroperoxone (EPO) process, a hybrid advanced oxidation technology combining electrochemical oxidation and ozonation. The results revealed that operational parameters, including current intensity, electrolyte concentration, ozone dosage, pH, and initial pollutant load, significantly influence degradation efficiency. Optimal removal performance was achieved at lower current intensities (250 mA) and mildly acidic pH (3–5), highlighting the importance of optimizing process conditions to balance efficiency and energy consumption.

Furthermore, machine learning algorithms were employed to model and predict the MO removal efficiency. Among the tested models, Random Forest outperformed Support Vector Regression, achieving a higher coefficient of determination ($R^2 = 0.823$) and a lower mean absolute error (MAE = 6.38), indicating superior predictive accuracy and robustness in capturing

nonlinear relationships among process variables.

The integration of experimental optimization and machine learning modeling offers a robust framework for advancing data-driven decision-making in water treatment technologies. Future work may focus on expanding the dataset, incorporating real wastewater matrices, and exploring hybrid ML models to further improve predictive performance and practical applicability.

Future research may focus on applying the EPO process to real wastewater samples, evaluating the formation of toxic by-products via LC-MS analysis, and scaling the process for semi-industrial or continuous-flow applications. The integration of real-time ML-based control strategies could further enhance system adaptability and performance.

References

- Abdi, J., Latifian, B., Firozjaee, T. T., & Hayati, B. (2025). Synthesis of magnetic PPAC@Fe3O4@MOF S-scheme heterojunction catalyst with enhanced removal of metronidazole antibiotic under visible light. *Journal of Water Process Engineering*, 72, 107540.
 - https://doi.org/https://doi.org/10.101 6/j.jwpe.2025.107540
- Bakheet, B., Yuan, S., Li, Z., Wang, H., Zuo, J., Komarneni, S., & Wang, Y. (2013). Electro-peroxone treatment of Orange II dye wastewater. *Water research*, 47(16), 6234-6243.
- Bopape, D. A., Ntsendwana, B., & Mabasa, F. D. (2024). Photocatalysis as a predischarge treatment to improve the effect of textile dyes on human health: A critical review. *Heliyon*, 10(20).
- Chaturvedi, A., Rai, B. N., Singh, R. S., & Jaiswal, R. P. (2022). A comprehensive review on the integration of advanced oxidation

- processes with biodegradation for the treatment of textile wastewater containing azo dyes. *Reviews in Chemical Engineering*, 38(6), 617-639.
- Chen, L., Wei, L., Ru, Y., Weng, M., Wang, L., & Dai, Q. (2023). A mini-review of the electro-peroxone technology for wastewaters: Characteristics, mechanism and prospect. *Chinese Chemical Letters*, 34(9), 108162.
- Deogaonkar-Baride, S., Koli, M., & Ghuge, S. P. (2025). Recycling Textile Dyeing Effluent through Ozonation: An Environmentally Sustainable Approach for reducing Freshwater and Chemical consumption and lowering Operational Costs. *Journal of Cleaner Production*, 145641.
- Fahimi Bandpey, A., Abdi, J., & Firozjaee, T. T. (2024). Improved estimation of dark fermentation biohydrogen robust production utilizing a categorical boosting machinelearning algorithm. International Journal of Hydrogen Energy, 52, 190-199.
 - https://doi.org/https://doi.org/10.101 6/j.ijhydene.2023.11.137
- Firozjaee, T. T., Mehrdadi, N., Baghdadi, M., & Bidhendi, G. N. (2020). Fixed-bed column study of diazinon adsorption on the cross-linked chitosan/carbon nanotube. *Environmental Engineering & Management Journal (EEMJ)*, 19(3), 467-474.
- Ghalebizade, M., & Ayati, B. (2016). Solar photoelectrocatalytic degradation of Acid Orange 7 with ZnO/TiO2 nanocomposite coated on stainless steel electrode. *Process Safety and Environmental Protection*, 103, 192-202.
 - https://doi.org/https://doi.org/10.1016/j.psep.2016.07.009
- Ghasemi, M., Khataee, A., Gholami, P., Soltani, R. D. C., Hassani, A., & Orooji, Y. (2020). In-situ electro-

generation and activation of hydrogen peroxide using a CuFeNLDH-CNTs modified graphite cathode for degradation of cefazolin. *Journal of Environmental Management*, 267, 110629.

https://doi.org/https://doi.org/10.1016/j.jenvman.2020.110629

- Khataee, A. R., Safarpour, M., Zarei, M., & Aber, S. (2011). Electrochemical generation of H2O2 using immobilized carbon nanotubes on graphite electrode fed with air: Investigation of operational parameters. *Journal of Electroanalytical Chemistry*, 659(1), 63-68.
 - https://doi.org/https://doi.org/10.101 6/j.jelechem.2011.05.002
- Lateef, S. A., Oyehan, I. A., Oyehan, T. A., & Saleh, T. A. (2022). Intelligent modeling of dye removal by aluminized activated carbon. *Environmental Science and Pollution Research*, 29(39), 58950-58962.
- Liu, C., Balasubramanian, P., Li, F., & Huang, H. (2024). Machine learning prediction of dye adsorption by hydrochar: Parameter optimization and experimental validation. *Journal of Hazardous Materials*, 480, 135853.
- Moosavi, S., Manta, O., El-Badry, Y. A., Hussein, E. E., El-Bahy, Z. M., Mohd Fawzi, N. f. B., Urbonavičius, J., & Moosavi, S. M. H. (2021). A study on machine learning methods' application for dye adsorption prediction onto agricultural waste activated carbon. *Nanomaterials*, 11(10), 2734.
- Naseri, S., & Ayati, B. (2024). Using green nanocomposite containing eggshell in the electroperoxone process in a baffled reactor to remove the

- emerging tetracycline pollutant. Environmental Research, 262, 119969.
- https://doi.org/https://doi.org/10.1016/j.envres.2024.119969
- Saghafi, S., Taghizade Firozjaee, T., Kardel, F., & Khoshnevisan, S. (2024). Modeling of Electrical Energy in Industrial Wastewater Treatment Plant with Traditional and Artificial Neural Network Approaches. *Journal of Hydraulic and Water Engineering*, 2(1), 112-125.
- Shahamat, Y. D., Masihpour, M., Borghei, P., & Rahmati, S. H. (2022). Removal of azo red-60 dye by advanced oxidation process O3/UV from textile wastewaters using Box-Behnken design. *Inorganic chemistry communications*, 143, 109785.
- Shokri, A., & Sanavi Fard, M. (2022). Employing electro-peroxone process for industrial wastewater treatment: a critical review. *Chemical Papers*, 76(9), 5341-5367.
- Tamer, T. M., Abbas, R., Sadik, W. A., Omer, A. M., Abd-Ellatif, M. M., & Mohy-Eldin, M. S. (2024). Development of novel amino-ethyl chitosan hydrogel for the removal of methyl orange azo dye model. *Scientific Reports*, 14(1), 1284.
- Tingting, S., Jiang, C. C., Wang, C., Sun, J., Wang, X.-k., & Li, X. (2015). A TiO2 modified abiotic–biotic process for the degradation of the azo dye methyl orange. *RSC Advances*, 5, 58704-58712.
- Wu, D., Lu, G., Zhang, R., Lin, Q., Yao, J., Shen, X., & Wang, W. (2017). Effective degradation of diatrizoate by electro-peroxone process using ferrite/carbon nanotubes based gas diffusion cathode. *Electrochimica Acta*, 236, 297-306.